# Analysis of human walking gait process and solution of the lower limb joint moment

Jun Yu

Zhongyuan-Petersburg Aviation College,
Zhongyuan University of Technology Zhengzhou, China
Email: 6523@zut.edu.cn

Shuaishuai Zhang*, Aihui Wang and Wei Li

School of Electric and Information Engineering,
Zhongyuan University of Technology,
Zhengzhou, China
Email: zss@zut.edu.cn
Email: a.wang@zut.edu.cn
Email: 2019006091@zut.edu.cn
*Corresponding author

**Abstract:** It is difficult to measure the characteristics of human limbs during movement, which leads to the complexity and inaccuracy of solving the mechanical properties of the joints. However, these unknown variables are essential for designing exoskeleton robots and cannot be ignored. Therefore, a rod model of the lower limb is identified in this paper, the different stages of human gait are discussed, and the interaction between the feet and the ground during human walking is analysed in detail. On this basis, the joint moment of lower limbs is deduced. Furthermore, inverse dynamic, net joint force, and moments for human lower limb joints are analysed theoretically. Finally, the principle of the high-fidelity Hill model is investigated, which verifies the feasibility and effectiveness of solving the net force and moment for human lower limb joints based on the plantar reaction force under certain circumstances theoretically. The research results of this paper will contribute to the field of lower limb exoskeleton robots and human lower limb prostheses.

**Keywords:** gait stages; ground reaction force; inverse dynamics; hill model; net joint force; joints moment.

**Reference** to this paper should be made as follows: Yu, J., Zhang, S., Wang, A. and Li, W. (2022) 'Analysis of human walking gait process and solution of the lower limb joint moment', *Int. J. Advanced Mechatronic Systems*, Vol. 9, No. 4, pp.211–218.

**Biographical notes:** Jun Yu received his PhD from the Nanjing University of Aeronautics and Astronautics, China, in 2012. He was an engineer in the 713th Research Institution of China Shipbuilding Industry Corporation during 2012 to 2016. He became a Lecturer in 2016 at the Zhongyuan University of Technology, China. His research interests include robust nonlinear control, smart materials-based actuators and bio-robot.

Shuaishuai Zhang obtained his Bachelor's degree from the Zhongyuan University of Technology, in 2019. Currently, he is a Master's student in the Zhongyuan University of Technology. His research interests include robust nonlinear control and bio-robot.

Aihui Wang received his PhD from the Tokyo University of Agriculture and Technology, Japan, in 2012. He became a Professor in 2021 at the Zhongyuan University of Technology, China. His research interests include robust nonlinear control, smart materials-based actuators and bio-robot.

Wei Li obtained his Bachelor's degree from the Henan University of Science and Technology in 2014. Currently, he is a Master's student in the Zhongyuan University of Technology.

## 1 Introduction

Modelling and simulating the human body through the biomechanics are important research contents in the development of wearable exoskeleton robots and prostheses. The research results of the motion state and biomechanical properties of human joints will guide the research and development of the wearable exoskeleton robot industry and human prosthetic products, promote the development of

Copyright © 2022 Inderscience Enterprises Ltd.

related research on human limb joints. Human lower limb modelling usually uses the connected rod model for analysis to simplify the uncertain factors of the analysis process, and perform model analysis according to relevant physical laws such as torque and acceleration. Finally, obtain the motion state of human joints and the net joints force and moment of the joints.

Chowdhury and Kumar (2013) studied the forces and moments acting on the hips and knees of the human lower limb joints. A method for estimating the joint force and moment of the lower limbs is proposed. This method uses a dynamic model to estimate the moment of the human ankle joint from the perspective of biomechanics (Chowdhury and Kumar, 2013). Deng and Wang (2012) established an IPMC nonlinear model for considering errors and designed an operator-based uncertainty control system for the model. The effectiveness of the method was verified by experiments and simulations (Deng and Wang, 2012). Compared with the energy consumption of the human lower limb model is driven by the net torque of muscles and joints theoretically. Experiments have verified that the models have small differences in the specific interval of the swing phase under different model driving methods (Prilutsky et al., 1996). A method is proposed to estimate the force generated by external and internal muscle activities of the hand and the influence of the force on the torque of the finger joints. Experimental studies have found that when the point of force changes from the far phalanx to the near interphalangeal joint, the given joint torque is reduced (Li et al., 2000). This paper provides a method for calculating the strength of the hip joints and knee joints on both sides of the bicycle during the human riding. This experiment compared the workload of six healthy subjects under different riding conditions and found that the bending load of the knee joints was basically constant and the maximum load of the lower limb joint when riding a bicycle was much smaller than that of walking and climbing stairs, (Ericson et al., 1986).

The subjects' average peak joint moments were analysed, and it was found that there was a certain correlation between the joint moments of the lower limbs, and there was coupling and interaction between them (Goldberg and Stanhope, 2013). Using wavelet neural network to establish a real-time proxy model to calculate the net moment of the lower limb joints, and compare it with the joint moments solved by traditional multi-body dynamics. Under the premise of ensuring the accuracy of the torque solution results, the calculation speed of the joint moments is improved (Ardestani et al., 2014). Wang and Deng (2013) proposed an uncertainty method based on operator theory to solve the uncertainty problem of the manipulator system, and established a robust nonlinear system to improve the tracking performance of the manipulator. A musculoskeletal model of the joint replacement complex was established in aaa, then combined with the actual motion characteristics of the hip joint, and the overall torque of the joint replacement was estimated by analysing the forces of ligaments and muscles and tendons, and compared with the results of the literature to verify the effectiveness of the established model. By analysing the joint torques and joint angles of the lower limbs of nine normal men walking at different speeds, the similarities and differences of human motion at different walking speeds are explained (Frigo et al., 1996). A simulation model of the assistive robot was established according to the changes in the torque of the lower limb joints of normal people, and the model was used to analyse the movement data of patients with limb dysfunction and normal people. It was found that the maximum torque of the hip joint was the largest, followed by the maximum torque of the knee joint, followed by the ankle joint (Kim et al., 2009).

The measurement of ground reaction force is the great significance in the biomechanical analysis of gait and other sports activities. Due to the differences in muscle activation and body movement, the ground reaction force changes vary between gaits. Then more motion information in human gait can be estimated through inverse dynamics. Veltink et al. (2005) installed force and torque sensors on shoes and measured the ground reaction force during walking combined with human gait characteristics. The changes in the ground reaction force help us understand the physical muscle activity and gait characteristics when walking. TEA Marasović et al. (2009a) used the AMTI platform to measure the ground reaction force and calculate the reaction force and muscle torque through motion analysis. When humans walk in normal gait, the ground reaction force of the left and right legs joint torque is similar, which also confirms the symmetry and periodicity of the normal gait. The speed of human walking has a huge impact on the ground reaction. To study the relationship between walking speed and ground reaction, Masani et al. (2002) measured the difference of ground reaction force on a treadmill. Their research results showed that there is an 'optimum speed' when walking, but it is only suitable for a treadmill-like propulsion control mechanism. However, the price of the force measurement platform is high, and it needs to build an independent collection space, so some researchers build a special neural network to predict the ground reaction force data. Oh et al. (2013) used artificial neural networks to predict the changes in the ground reaction force during the dual-support phase and they obtained the similar results to those measured by the force measurement platform. When the musculoskeletal model is used to study the human motion state, the data collected by the force measurement platform has a certain degree of uncertainty and the mismatch between the model and the collected object will increase the difficulty of inverse dynamic analysis. The development of sensor technology makes it possible to measure the characteristics of the body movement process. According to the collected force plate data, the left and right leg moments of 40 subjects were analysed and compared, and the corresponding characteristic comparison results were obtained (Marasović et al., 2009b).

The change of joint moment in human gait motion is a complicated process, which is not only related to the established human model but also closely related to the

fidelity of the model. Inaccurate models will cause high errors in model analysis. Therefore, it is a great practical significance to establish a suitable human body model and derive the moment changes in human gait based on the model. For example, obtaining the forces and moments of the joints of the lower limbs is helpful for the quantification of lower limb exoskeleton robots and the development of lower limb prostheses.

This paper first divides the movement stages of human gait, as described in Section 2. Section 3, focuses on the interaction between the sole and the ground during walking, analyses the changes in the reaction force of the sole, and paves the way for subsequent chapters. Section 4 is a continuation of Section 3. In Section 4, this paper introduces the derivation and calculation of the net force and moment of the human lower limb joints in detail. Finally, in Section 5, the principles of high-fidelity musculoskeletal model modelling are analysed.

## 2 Ground reaction forces

### *2.1 Classification of Gait Stages*

The division of the gait phase is shown in Figure 1, the division of the gait phase starts from the initial contact of the sole. The supporting phase refers to the phase where the foot touches the ground and bears gravity during walking. The 1–5 in Figure 1 represents the support phase, and the numbers represent the pre-support period, early support phase, mid-support phase, late support phase, and end support phase, accounting for 60% of the gait cycle. The swing phase refers to the phase when the feet leave the ground and swing under the traction of the legs during walking. In the figure, 6–8 represent the swing phases, and the numbers respectively represent the initial swing, the middle swing, and the end swing, which account for 40% of the gait cycle.

**Figure 1** Division of gait stages (see online version for colours)

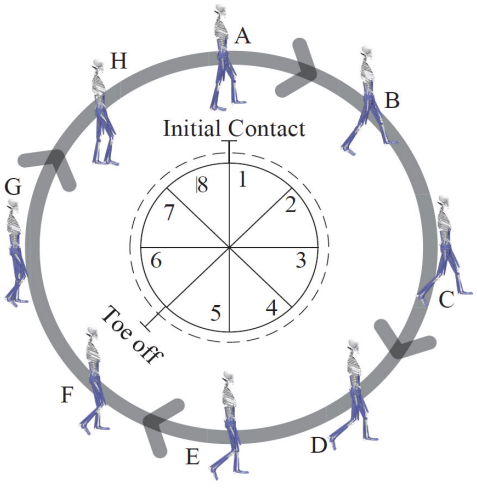


The gait cycle describes refer to the changes of the left foot and left leg. Where, A: initial contact, left heel touches the ground. B: load response, touch the ground with left foot. C: heel off, left foot support. D: opposite initial contact, left heel off the ground. E: toe off, left toe off the ground. F: feet adjacent, before the left leg swings. G: Tibia vertical, swinging the left leg. H: prepare initial contact, after the left leg swings.

### *2.2 Human gait reaction forces analysis*

In the normal walking process, the interaction with the external environment only has the force of the sole after ignoring the influence of friction and so on. Therefore, the reaction force of the sole is very important in the study of gait. To obtain the change of the interaction force between the human and the ground during walking, this paper starts from the force plate data to study the force interaction between the foot and the ground. The data collected by the force plate is the reaction force of the ground to the sole. As described in Newton's second theorem, force is the cause of the acceleration of the centre of mass of an object at every moment, and force changes the object's state of motion. Therefore, this paper links the external force of human motion with the acceleration of the object.

### *2.3 Vertical direction of ground reaction force*

As shown in Figure 2, it is the vertical component of the ground reaction force, the abscissa represents the percentage of the gait cycle, and the vertical axis represents the ratio of the plantar reaction force to the weight of the subject.

**Figure 2** Ground reaction forces in vertical axis (see online version for colours)

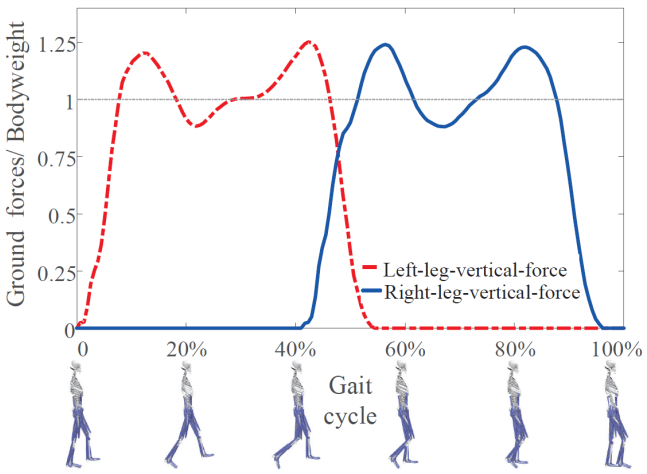


The vertical component of the ground reaction force rises rapidly after the sole touches the ground. This rise is to offset the inertial impact from the previous step, that is, to prevent the body from falling forward. Gravity, which reaches body weight at about 8% of the gait cycle, begins to enter the overweight stage, and reaches the apex of the overweight state at 12%. The overweight state at this time is equivalent to 1.24 times the acceleration of gravity. Then it returns to the normal value of weight and gravity at 18% of the gait cycle, and then enters the state of weightlessness. At 22% of the gait cycle, the weightlessness of the body drops

to the lowest point. Weightlessness is equivalent to 0.8 times of body weight, and then it will enter the weightlessness recovery phase, returning to the normal value of weight and gravity at 28%. Finally, it enters the overweight stage. At this time, the overweight is to provide the body with an upward and forward force, which provides the body with forwarding power. The driving power from the ground reaction force reaches its peak in 42% of the gait cycle. Which is 1.25 times the weight of normal weight.

It can be seen that almost at the moment when the power leg provides the maximum power, the other leg starts to participate, the single support phase ends, and the double support phase is entered. The newly added leg is buffered to offset the excess provided by the previous leg. At the same time, keep the body stable to ensure that the body does not fall. Then, the vertical force of the front leg quickly drops to zero, and the leg vacates off the force plate. So far, one step of walking is completed, and the subsequent gait will repeat this process to achieve continuous gait walking. In the whole process, only when the body's gravity is equal to the force in the vertical direction of the force plate, the centre of mass has no static vertical acceleration. When walking at a normal pace, there are two peaks in the vertical ground reaction force during the entire gait process, which appear at the position where the impact is buffered after contact with the ground and the position where it provides power for the next step. The peaks of these two peaks are almost equal. During the period, the energy lost due to exercise is supplemented by the muscles, and the siege walk continues.

### *2.4 Horizontal direction of ground reaction force*

As shown in Figure 3, it is the horizontal component of the ground reaction force, including the front-to-back direction and the left-right direction. The abscissa represents the percentage of the gait cycle, and the vertical axis represents the ratio of the plantar reaction force to the weight of the subject.

**Figure 3** Ground reaction forces in horizon X and Z axes (see online version for colours)

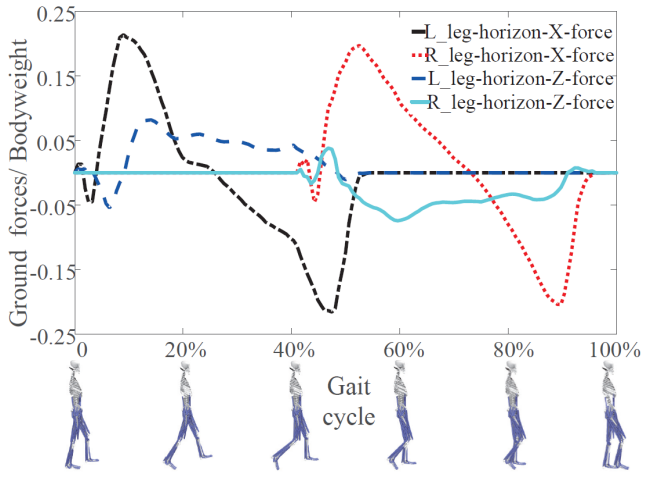


Compared with the force in the vertical direction, the force in the horizontal forward direction is a relatively small force, which is used to buffer and maintain stability, and at the same time provide the power for the next step forward through the frictional force. The horizontal ground reaction force has a backward force (pointing to the back of the body) at the initial stage when the sole touches the force plate, which is used to buffer the force in the horizontal forward direction during the previous step of walking. This force almost reaches the maximum amplitude before and after the vertical force reaches the highest peak, and then slowly returns to zero, enters the single support stage, and is used to provide forward movement power through the friction of the sole. The force changes direction, change into the direction of progress, and slowly return to zero after providing forward power (basically completing the mission of this step).

There is also a smaller left-right force in the horizontal direction. Although this force is small, it is indispensable for controlling the body's left-right balance. In addition, a gait with a larger step width is usually caused by a larger toe extension. To maintain balance, it may be necessary to increase the step width to reduce the risk of falling. The horizontal force is used to counteract downward gravity and help regulate walking speed. When both feet are in contact with the ground (dual support phase), we must add up the forces acting on each foot. The front-to-back force of the front foot needs to offset the back-to-front force of the back foot to prevent the faster going, the back foot advances, and the front foot brakes.

## 3 Inverse dynamics analysis

Inverse dynamics refers to the inverse calculation of the internal state parameters of the object from the external performance of the moving object. In this section, based on the collected ground reaction force during the gait process, combined with the principle of inverse dynamics, the net joints force and moments derivation process of the ankle joint, knee joint, and hip joint is obtained. Since there is no contact between the soles of the feet and the ground in the swing phase, the force plate cannot be used to obtain any torque information at this stage. Therefore, this derivation is only applicable to the gait stages where the soles of the feet are in contact with the ground. In this derivation, the human body segment is re-divided into four rigid body segments: foot, calf, thigh, upper limbs, and torso (as a whole), and sports joints include ankle, knee, and hip. The supporting phase of the gait process is shown in Figure 4. Starting from the foot, based on the collected force plate data, the net force and moment of the joint force are analysed and solved.

Where, $m_1$, $m_2$, $m_3$ are the masses of the lower leg, thigh and upper body respectively; $I_1$, $I_2$, $I_3$ are the inertia moment of the lower leg, thigh and upper body respectively; $\theta_1$, $\theta_2$, $\theta_3$ are the joint angles of the ankle, knee and hip joints respectively; $l_1$ and $l_2$ are the length of the lower leg and thigh, respectively; $r_1$ is the distance from the centre of mass of the lower leg to the ankle, $r_2$ is the distance from the centre of mass of the thigh to the knee joint, $r_3$ is the

distance from the centre of mass of the upper body to the hip joint.

In this part, we first establish a three-dimensional rectangular coordinate system. This coordinate system is different from our common Z-axis representing up and down coordinate systems. In this coordinate system, the Y-axis represents up and down, and the X-axis represents the direction of forward and backward. In the plane direction, the Z-axis represents the left and right directions.

**Figure 4** Sketch of the human body connecting rod model (see online version for colours)

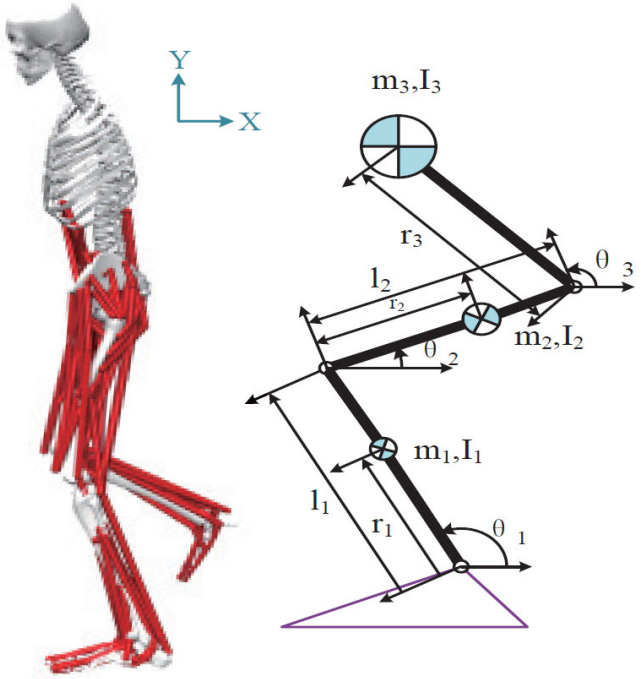


**Figure 5** Moments analysis for the foot segment of the model (see online version for colours)

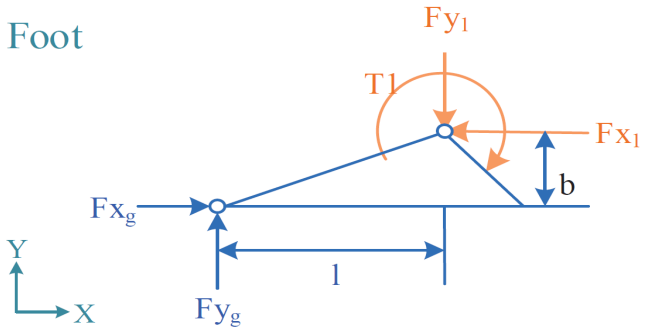


The coordinate definition of the foot rigid body is shown in Figure 5. Use Newton's second law equation (1) for mechanical analysis. Where, b and l are the lengths to be measured, and $F_{xg}$ and $F_{yg}$ are the ground reaction forces to be measured. Unknown quantities include plantar reaction forces $F_{x1}$ and $F_{y1}$, and ankle joint torque $T1$.

$$\sum F = m_0 \ddot{x}_0 \tag{1}$$

where $m_0$ is the mass of foot segment, $Fx$* is the force in $X$ axis, $Fy$* is the force in $Y$ axis. In the gait support phase, the sole of the foot does not leave the ground. At this time, the foot remains still, the acceleration of $\ddot{x}_0$ is 0, and the resultant external force is 0, so the equation (2) is satisfied. The resultant force in the axial direction is zero, and in the same way, it can be satisfied in the X-axis direction equation (3).

$$Fy_1 = Fy_g \tag{2}$$

$$Fx_1 = Fx_g \tag{3}$$

### *3.1 Ankle joint force and moment solution*

When calculating the rotational moment of an object about a certain point, it generally has the following form, based on which the ankle joint moment $T1$ in Figure 5 can be solved.

$$\sum M_{\mathrm{P}} = I\ddot{\theta} + \left(\underline{r}^{\mathrm{P}} \times m\underline{a}\right) \cdot \hat{z} \tag{4}$$

where $\sum M_{\mathrm{P}}$ represents the sum of moments at the point $P$, $I$ represents the moment of inertia of an object around the centre of mass, $\underline{r}^{\mathrm{P}}$ represents the vector from point P to the centre of mass, $\underline{a}$ represents the linear acceleration for the centre of mass of the object.

Since the sum moment is zero, that is, $\sum M_{\mathrm{P}}$ is equal to 0, get:

$$Fx_g h - Fy_g \ell - T_1 = \mathrm{o}.$$

Then get the ankle moment as:

$$T_1 = Fx_g h - Fy_g \ell \tag{5}$$

### *3.2 Knee joint force and moment solution*

The definition of the rigid body coordinates of the calf is shown in Figure 6, where the measurement includes: $l_1$ and $r_1$ length, $\theta_1$ the angle between the calf and the horizontal plane at this time, $m_1$ is the mass of the calf, $I_1$ the moment of inertia of the calf. The calculated quantities include: ankle joint forces $Fx_1$ and $Fy_1$, and ankle torque $T_1$. Unknown quantities include $Fx_2$ and $Fy_2$, and torque $T_2$. Let the coordinates of the centroid position of the calf be $(x_1, y_1)$.

**Figure 6** Moments analysis for the shank segment of the model (see online version for colours)

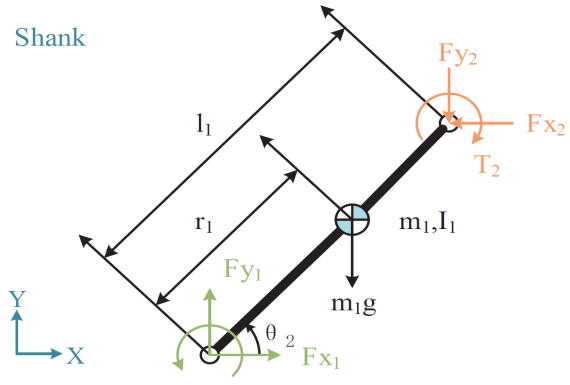

Available from the knowledge of dynamics:

$$x_1 = r_1 \cos\theta_1 \tag{6}$$

$$\ddot{x}_1 = -r_1\left(s\theta_1\ddot{\theta}_1 + c\theta_1\dot{\theta}_1^2\right) \tag{7}$$

$$y_1 = r_1\, s\theta_1 \tag{8}$$

$$\ddot{y}_1 = r_1\left(\cos\theta_1\ddot{\theta}_1 - \sin\theta_1\dot{\theta}_1^2\right) \tag{9}$$

Use Newton's second theorem in the $X$ and $Y$ direction to get:

$$Fx_1 - Fx_2 = -m_1 r_1\left(\sin\theta_1\ddot{\theta}_1 + \cos\theta_1\dot{\theta}_1^2\right) \tag{10}$$

$$Fy_1 - Fy_2 - m_1 g = m_1 r_1\left(\cos\theta_1\ddot{\theta}_1 - \sin\theta_1\dot{\theta}_1^2\right) \tag{11}$$

Finally, the torque balance condition at the centre of mass is obtained:

$$\begin{aligned} &T_1 - T_2 + Fx_1 r_1 \sin\theta_1 - Fy_1 r_1 \cos\theta_1 \\ &+Fx_2 d_1 \sin\theta_1 - Fy_2 d_1 \cos\theta_1 = I_1\ddot{\theta}_1 \end{aligned} \tag{12}$$

Among them, $d_1 \triangleq \ell_1 r_1$, combining the three formulas [equation (10), equation (11), equation (12)] can solve the force and moment acting on the knee joint.

### 3.3 *Hip joint force and moment solution*

The definition of the rigid body coordinates of the thigh is shown in Figure 7, where the measurement includes: $l_2$ and $r_2$ length, $\theta_2$ the angle between the thigh and the horizontal plane at this time, $m_2$. The mass of the thigh, $I_2$ the moment of inertia of the thigh. The calculated quantities include knee joint forces $Fx_2$ and $Fy_2$, torque $T_2$. Unknown quantities include hip joint forces $Fx_3$ and $Fy_3$, and torque $T_3$. Let the coordinates of the centre of mass of the thigh be $(x_2, y_2)$.

**Figure 7** Moments analysis for the thigh segment of the model (see online version for colours)

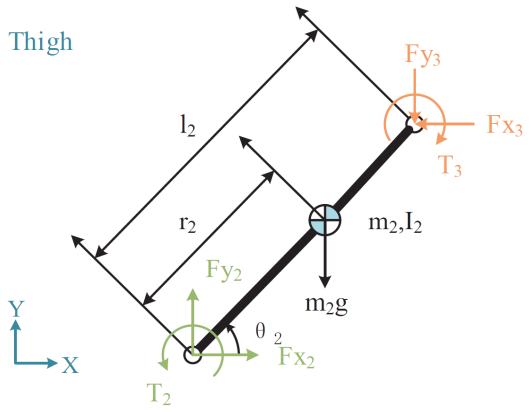


From the knowledge of kinetics:

$$x_2 = \ell_1 \cos\theta_1 + r_2 \cos\theta_2 \tag{13}$$

$$\begin{aligned} \ddot{x}_2 = &-\ell_1\left(\sin\theta_1\ddot{\theta}_1 + \cos\theta_1\dot{\theta}_1^2\right) \\ &-r_2\left(\sin\theta_2\ddot{\theta}_2 + \cos\theta_2\dot{\theta}_2^2\right) \end{aligned} \tag{14}$$

$$y_2 = \ell_1 \sin\theta_1 + r_2 \sin\theta_2 \tag{15}$$

$$\begin{aligned} \ddot{y}_2 = &\ell_1\left(\cos\theta_1\ddot{\theta}_1 - \sin\theta_1\dot{\theta}_1^2\right) \\ &+r_2\left(\cos\theta_2\ddot{\theta}_2 - \sin\theta_2\dot{\theta}_2^2\right) \end{aligned} \tag{16}$$

Use Newton's second theorem in the $X$ and $Y$ direction to get:

$$F_{x_2} - F_{x_3} = m_2\ddot{x}_2 \tag{17}$$

$$F_{y_2} - F_{y_3} - m_2 g = m_2\ddot{y}_2 \tag{18}$$

Finally, the torque balance condition at the centre of mass is obtained,

$$\begin{aligned} &T_2 - T_3 + F_x r_2 \sin\theta_2 - F_{y_2} r_2 \cos\theta_2 \\ &+F_{x_3} d_2 \sin\theta_2 - F_{y_3} d_2 \cos\theta_2 = I_2\ddot{\theta}_2 \end{aligned} \tag{19}$$

where $d_2 \triangleq \ell_2 r_2$, combining the three formulas [equation (14), equation (16), equation (19)] can solve the force and moment acting on the hip joint.

**Figure 8** Moments analysis for the upper limbs and torso of the model (see online version for colours)

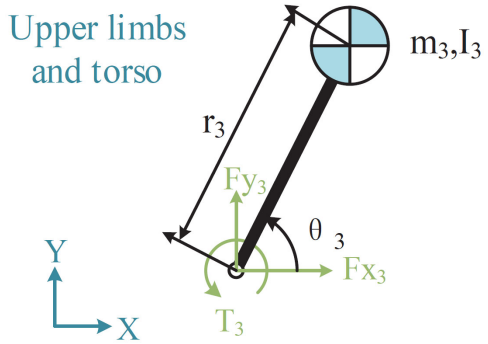


This paper mainly studies the dynamics and kinematics analysis related to the human lower limbs. For this reason, in the formula derivation, this paper simplified the part above the waist into a whole rigid body, as shown in Figure 8. So far, the derivation of the net forces and moments of the hip, knee, and ankle joints has been completed. This derivation will help the research of this paper to obtain theoretical support for the calculation data.

## 4 Hill-type muscle model

A musculoskeletal model of a specific subject is established based on the biological characteristics of the human body's lower limbs and measured data of equidistant points, and an optimisation method for optimising muscle and tendon parameters is proposed, which has good results (Heinen et al., 2019). Michaud and Begon (2021) proposed a multi-data fusion algorithm to fuse the collected human biological characteristic data and make full use of the various data that can be collected to obtain muscle simulation. A model system of human hands that interacts between the arm and the mechanical arm was developed. The system can track the arm of the rehabilitation robot to

simulate a normal human hand. In all the tester tests, the error reached less than 5 mm (Ayodele et al., 2021).

Muscle stimulation is often used to study motion dynamics. Muscle simulation mainly uses muscle and tendon models for driving simulation. Millard et al. (2013) compared the speed and accuracy of three common muscle models, and the results show that the balance model is better. Zhang et al. (2021) proposed an artificial muscle control method to control muscle contraction and relaxation, tested the model's accuracy through experiments, and obtained good test results. The human modelling theory of OpenSim is mainly derived from the Hill equation and Hill muscle model. Hill-type muscle model contains three muscle elements, namely contractile element (CE), series elastic element (SE), and parallel elastic element (PE). OpenSim's hill-type muscle model, which converts activation signals into muscle forces, including the force-length($f_{FL}(L_{CE})$) and force-velocity ($f_{FV}(\dot{L}_{CE})$) properties of muscles. Hill-type muscle model is shown in Figure 9.

**Figure 9** Hill-type muscle models

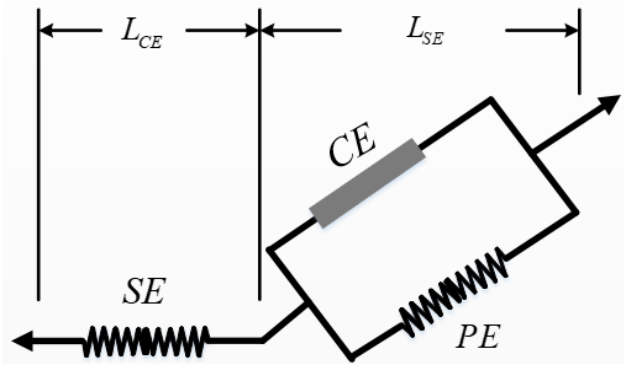


Reference to Figure 9. Where, $L_M$ is the total length of the muscle. $L_{SE}$ is the length of the SE. For the SE and PE parts, we have established a nonlinear spring model.

$$f_{spring} = \begin{cases} k_1(l - l_s) & l \le l_s \\ k_1(l - l_s) + k_2(l - l_s)^2 & l > l_s \end{cases} \tag{20}$$

where $l$ represents the total length of the spring when it is deformed. $l_s$ is the static length of the spring without force. $k_1$ and $k_2$ is the coefficient of the spring, which is related to the characteristics of the spring itself.

According to the research results of Pandy et al. (2004), we can get the muscle strength (FCE) produced by CE in Hill-type muscle model.

$$F_{CE} = aF_{\max} f_{FL}(L_{CE}) f_{FV}(\dot{L}_{CE}) \tag{21}$$

where $a$ is the activation signals, $F_{\max}$ is the maximal isometric force. On the one hand, we can get $f_{FL}(L_{CE})$ and $f_{FV}(\dot{L}_{CE})$ through Opensim software; on the other hand, we adopt an approximate method to determine the value of them.

$$f_{FL} = \exp\left(-\left(\frac{L_{CE} - L_{CEopt}}{WL_{CEopt}}\right)^2\right) \tag{22}$$

$$f_{FV} = \begin{cases} \dfrac{V_{\max} + V_{CE}}{V_{\max} - \dfrac{V_{CE}}{A}} V_{CE} \le 0 \\ \dfrac{g_{\max} V_{CE} + c}{V_{CE} + c} V_{CE} > 0 \end{cases} \tag{23}$$

where $L_{CEopt}$ is a muscle-dependent constant termed the optimal CE length. $W$ is the parameter of the force-engtth curve. $g_{\max}$ is the maximal normalised eccentric muscle force, and c is a muscle-dependent constant, $V_{\max}$ is the maximum shortening velocity at full activation. We use the angle of the joint driven by the muscle to express the fibre length of the muscle (Sartori et al., 2012).

$$L_{CE}(\theta) = a_0 + a_1\theta + a_2\theta^2 + a_3\theta^3 \tag{24}$$

where $\theta$ is the angle of the joint, $a_1 \sim a_3$ are the coefficient of the polynomial.

The state equation for the muscle is the force balance equation for the three element structure:

$$(F_{CE} + F_{PE})\cos\varphi = F_{SE} \tag{25}$$

$F_{CE}$, $F_{SE}$ and $F_{PE}$ are the muscle power produced by *CE*, *SE* and *PE*, respectively. $\varphi$ is the angle between the longitudinal axis of the muscle mass and its constituent fibres.

The model can be adopted to simulate the musculoskeletal model, obtain the maximum equidistant force and joint torque that can be generated at any position, and study the ability of different muscles to generate torque. Then generate muscle driving signals during walking or running, and analyse muscle's contribution to movement. Each segment of the model has a fixed frame of reference.

## 5 Conclusions

This paper evaluates the net joint force and joint moment of each lower limb joint during walking objectively. Then it provides a feasible scheme for the estimation and solution of the net joint force and joint moment of the human lower limb joints. This estimation can be used to study the relevant characteristics of the joints during the exercise and provided a certain reference for the development of human lower limb prostheses. This paper obtains information about joints of the human lower limbs based on normal human movement that applies to control and optimisation of the lower limb prostheses. Finally, achieve prosthetic tracking and imitate the movement of normal limbs. Meanwhile, this research will provide a certain reference for the clinical gait analysis of the lower limbs rehabilitation patients significantly, and also help patients with lower limbs dysfunction to return the normal life.

In addition, the change process of the plantar reaction force in the different phases is studied during human walking. The law of the moment change of the human body

movement during walking is obtained by studying the changes in the ratio of the plantar reaction force to the weight of the subject during the asynchrony phase. Then, combined with the rigid body model and theoretical analysis of the lower limbs, the forces and moments of the ankle, knee, and hip joints are obtained by the inverse solution of the plantar reaction force, the solution process is deduced and calculated theoretically. Finally, the modelling principle of a high-fidelity muscle model is analysed and deduced theoretically, and the feasibility of the muscle modelling method is proved theoretically. This paper provides some help for the research of lower limb kinematics and the development of lower limb prostheses.

## Acknowledgements

The project is funded in part by the National Institutes of Health, under Grant No. 5R01CA136535.

## References

Ardestani, M.M., Zhang, X., Wang, L., Lian, Q., Liu, Y., He, J., Li, D. and Jin, Z. (2014) 'Human lower extremity joint moment prediction: a wavelet neural network approach', *Expert Systems with Applications*, Vol. 41, No. 9, pp.4422–4433.

Ayodele, K.P., Akinniyi, O.T., Oluwatope, A.O., Jubril, A.M., Ogundele, A.O. and Komolafe, M.A. (2021) 'A simulator for testing planar upper extremity rehabilitation robot control algorithms', *Nigerian Journal of Technology*, Vol. 40, No. 1, pp.115–128.

Chowdhury, S. and Kumar, N. (2013) 'Estimation of forces and moments of lower limb joints from kinematics data and inertial properties of the body by using inverse dynamics technique', *Journal of Rehabilitation Robotics*, Vol. 1, No. 2, pp.93–98.

Deng, M. and Wang, A. (2012) 'Robust nonlinear control design to an ionic polymer metal composite with hysteresis using operator based approach', *IET Control Theory & Applications*, Vol. 6, No. 17, pp.2667–2675.

Ericson, M.O., Bratt, A., Nisell, R., Nemeth, G. and Ekholm, J. (1986) 'Load moments about the hip and knee joints during ergometer cycling', *Scandinavian Journal of Rehabilitation Medicine*, Vol. 18, No. 4, pp.165–172.

Frigo, C., Crenna, P. and Jensen, L.M. (1996) 'Moment-angle relationship at lower limb joints during human walking at different velocities', *Journal of Electromyography and Kinesiology*, Vol. 6, No. 3, pp.177–190.

Goldberg, S.R. and Stanhope, S.J. (2013) 'Sensitivity of joint moments to changes in walking speed and body-weight-support are interdependent and vary across joints', *Journal of Biomechanics*, Vol. 46, No. 6, pp.1176–1183.

Heinen, F., Sørensen, S.N., King, M., Lewis, M., Lund, M.E., Rasmussen, J. and Zee, M. (2019) 'Muscle-tendon unit parameter estimation of a Hill-type musculoskeletal model based on experimentally obtained subject-specific torque profiles', *Journal of Biomechanical Engineering*, Vol. 141, No. 6, pp.061005–061014.

Kim, S.M., Lee, S.Y., Kang, H.C. and Jeong, J.H. (2009) 'Study of knee and hip joints' moment estimation by biomechanical simulation during various motion changes', in *Proceedings of the World Congress on Engineering and Computer Science*, October.

Li, Z.M., Zatsiorsky, V.M. and Latash, M.L. (2000) 'Contribution of the extrinsic and intrinsic hand muscles to the moments in finger joints', *Clinical biomechanics*, Vol. 15, No. 3, pp.203–211.

Marasović, T., Cecić, M. and Zanchi, V. (2009a) 'Analysis and interpretation of ground reaction forces in normal gait', *WSEAS Transactions on Systems*, Vol. 8, No. 9, pp.1105–14.

Marasović, T., Cecić, M. and Zanchi, V. (2009b) 'Ground reaction forces in gait: Statistical analysis and interpretation', *WSEAS Trans. Syst.*, Vol. 8, No. 9, pp.1105–1114.

Masani, K., Kouzaki, M. and Fukunaga, T. (2002) 'Variability of ground reaction forces during treadmill walking', *Journal of Applied Physiology*, Vol. 92, No. 5, pp.1885–1890.

Michaud, B. and Begon, M. (2021) 'biorbd: a C++, Python and MatLab library to analyze and simulate the human body biomechanics', *Journal of Open Source Software*, Vol. 6, No. 57, pp.2562–2567.

Millard, M., Uchida, T., Seth, A. and Delp, S.L. (2013) 'Flexing computational muscle: modeling and simulation of musculotendon dynamics', *Journal of Biomechanical Engineering*, Vol. 135, No. 2, pp.021005–021016.

Oh, S.E., Choi, A. and Mun, J.H. (2013) 'Prediction of ground reaction forces during gait based on kinematics and a neural network model', *Journal of Biomechanics*, Vol. 46, No. 14, pp.2372–2380.

Pandy, M.G., Barr, R.E. and Kutz, M. (2004) 'Biomechanics of the musculoskeletal system', *Standard Handbook of Biomedical Engineering and Desing*.

Prilutsky, B.I., Petrova, L.N. and Raitsin, L.M. (1996) 'Comparison of mechanical energy expenditure of joint moments and muscle forces during human locomotion', *Journal of Biomechanics*, Vol. 29, No. 4, pp.405–415.

Sartori, M., Reggiani, M., van den Bogert, A.J. and Lloyd, D.G. (2012) 'Estimation of musculotendon kinematics in large musculoskeletal models using multidimensional B-splines', *Journal of Biomechanics*, Vol. 45, No. 3, pp.595–601.

Veltink, P.H., Liedtke, C., Droog, E. and van der Kooij, H. (2005) 'Ambulatory measurement of ground reaction forces', *IEEE Transactions on Neural Systems and Rehabilitation Engineering*, Vol. 13, No. 3, pp.423–427.

Wang, A. and Deng, M. (2013) 'Robust nonlinear multivariable tracking control design to a manipulator with unknown uncertainties using operator-based robust right coprime factorization', *Transactions of the Institute of Measurement and Control*, Vol. 35, No. 6, pp.788–797.

Zhang, Q., Yang, M., Shen, X., Tian, M. and Wang, X. (2021) 'Muscle-like contraction control of tendon-sheath artificial muscle', *Mechatronics*, Vol. 77, No. 2021, pp.102584–102593.